

A System for Indoor Guidance Using Visible Light Communication

Manuela Vieira, Manuel Augusto Vieira, Paula Louro,
Alessandro Fantoni
ADETC/ISEL/IPL,
R. Conselheiro Emídio Navarro, 1959-007
Lisboa, Portugal
CTS-UNINOVA
Quinta da Torre, Monte da Caparica, 2829-516,
Caparica, Portugal

e-mail: mv@isel.ipl.pt, mv@isel.pt, plouro@deetc.isel.pt,
afantoni@deetc.isel.ipl.pt

Pedro Vieira
ADETC/ISEL/IPL,
R. Conselheiro Emídio Navarro, 1959-007
Lisboa, Portugal
Instituto das Telecomunicações
Instituto Superior Técnico, 1049-001,
Lisboa, Portugal
e-mail: pvieira@isel.pt

Abstract— Communications within personal working/living spaces are highly demanded. To support people’s wayfinding activities, we propose a Visible Light Communication (VLC) cooperative system that supports guidance services and uses an edge/fog-based architecture for wayfinding services. A mesh cellular hybrid structure is proposed. The dynamic navigation system is composed of several transmitters (ceiling luminaries), which send the map information and path messages required to wayfinding. The luminaires are equipped with one of two types of nodes: a “mesh” controller that connects with other nodes in its vicinity and can forward messages to other devices in the mesh, effectively acting like routers nodes in the network and a “mesh/cellular” hybrid controller, that is also equipped with a modem providing IP base connectivity to the central manager services. These nodes act as border-router and can be used for edge computing. Mobile optical receivers, using joint transmission, collect the data at high frame rates, extracts their location to perform positioning and, concomitantly, the transmitted data from each transmitter. Each luminaire, through VLC, reports its geographic position and specific information to the users, making it available for whatever use. Bidirectional communication is implemented and the best route to navigate through venue calculated. The results show that the system makes possible not only the self-localization, but also to infer the travel direction and to interact with information received optimizing the route towards a static or dynamic destination.

Keywords- Visible Light Communication; Indoor navigation; Bidirectional Communication; Wayfinding; Optical sensors; Indoor multi-level environments; Transmitter/Receiver.

I. INTRODUCTION

This paper is an extended version from the one presented in ALLSENSORS 2022 [1].

Nowadays, wireless networks have seen a demand for increased data rate requirements. For a realistic coverage with the data rate requirements, a large bandwidth is needed which remains a limiting factor when compared with the RF communication technologies. Consequently, research has started exploring alternate wireless transmission

technologies to meet the ever-increasing demand. In this context, the huge bandwidth available in the unlicensed electromagnetic spectrum in the optical domain is seen as a promising solution to the spectrum crunch.

Visible Light Communication (VLC) makes use of the higher frequencies in the visual band and extends the capabilities of data transmission using general light sources. VLC has been regarded as an additional communication technology [2] [3] to fulfill the high data rate demands and as a new affiliate in the beyond fifth generation (5G) heterogeneous networks. It can be easily used in indoor environments using the existing LED lighting infrastructure with few modifications [4] [5]. Research has shown that compared to outdoors, people tend to lose orientation a lot easier within complex buildings [6] [7]. Fine-grained indoor localization can be useful, enabling several applications [8] [9].

This work focuses on the use of VLC as a support for the transmission of information, providing advertising services and specific information to users. The goal is a cooperative system that supports guidance services and uses an edge/fog based architecture for wayfinding services. Here, the luminaire, through VLC, reports its geographical positions and specific information to the users since its infrastructure can also be reused to embed the fog nodes in them. The system is composed of several transmitters (LEDs luminaries), which send the map information and path messages required to wayfinding. Data is encoded, modulated and converted into light signals emitted by the transmitters. Every mobile terminal is equipped with a receiver module for receiving the mapped information generated from the ceiling light and displays this information in the mobile terminal. The receiver module includes a photodetector based on a tandem a-SiC:H/a-Si:H pin/pin light-controlled filter [10] [11].

Visible light can be used as an ID system and can be employed for identifying the room number and the building itself. The main idea is to divide the service area into spatial

beams originating from the different ID light sources and identify each beam with a unique timed sequence of light signals. The signboards, based on arrays of LEDs, positioned in strategic directions to broadcast the information [12], are modulated acting as down- and up-link channels in the bidirectional communication. For the consumer services, the applications are enormous. The objective is to allow the implementation of new services in these areas using data from the VLC System, for indoor and outdoor. Positioning, navigation, security and even mission critical services are possible use cases that should be implemented.

In this paper, a LED-supported guidance VLC system is proposed. After the Introduction, in Section II, the communication system is described. In Section III, the main experimental results are presented, downlink and uplink transmission is implemented and the best route to navigate calculated. In Section IV, the conclusions are drawn.

II. COMMUNICATION SYSTEM, DESIGN AND ARCHITECTURE

The main goal is to specify the system conceptual design and define a set of use cases for a VLC based guidance system to be used by mobile users inside large buildings.

A. Communication system and cooperative localization

The system is composed by two modules: the transmitter and the receiver.

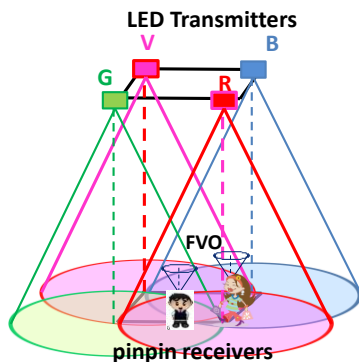
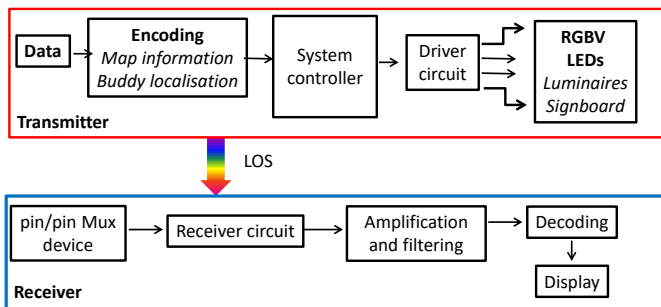


Figure 1. Block diagram and transmitters and receivers 3D relative positions.

The block diagram and the transmitter and receiver relative positions are presented in Figure 1. Both communication modules are software defined, where modulation/ demodulation can be programed.

Data from the sender is converted into an intermediate data representation, byte format, and converted into light signals emitted by the transmitter module. The data bit stream is input to a modulator where an ON-OFF Keying (OOK) modulation is utilized. On the transmission side, a modulation and conversion from digital to analog data is done. The driver circuit will keep an average value (DC power level) for illumination, combining it with the analog data intended for communication. The visible light emitted by the LEDs passes through the transmission medium and is then received by the MUX device.

To realize both the communication and the building illumination, white light tetra-chromatic sources are used providing a different data channel for each chip. Each luminaire is composed of four white LEDs framed at the corners of a square (Figure 2). At each node, only one chip of the LED is modulated for data transmission, the Red (R: 626 nm), the Green (G: 530 nm), the Blue (B: 470 nm) or the Violet (V). In Figure 2a, the spectra of the input channels is displayed.

Data is encoded, modulated and converted into light signals emitted by the transmitters. Modulation and digital-to-analog conversion of the information bits is done using signal processing techniques.

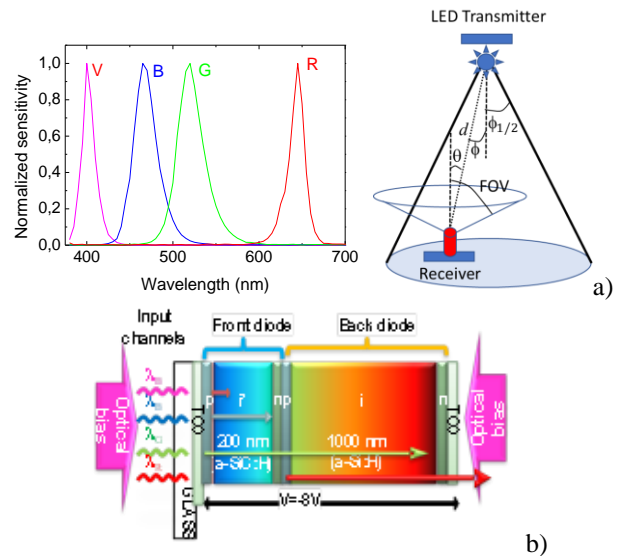


Figure 2. a) Spectra of the input channels. b) Configuration and operation of the pin/pin Mux device.

The signal is propagating through the optical channel, and a VLC receiver, at the reception end of the communication link, is responsible to extract the data from the modulated light beam. It transforms the light signal into an electrical signal that is subsequently decoded to extract the transmitted information. The obtained voltage is then

processed, by using signal conditioning techniques (adaptive bandpass filtering and amplification, triggering and demultiplexing), until the data signal is reconstructed at the data processing unit (digital conversion, decoding and decision) [13] [14]. At last, the message will be output to the users.

In the receiving system, a MUX photodetector acts as an active filter for the visible spectrum. The VLC photosensitive receiver is a double pin/pin photodetector based on a tandem heterostructure, p-i-n/p-i-n sandwiched between two conductive transparent contacts (Figure 2a). The front, thin pi'n structure made of a-SiC:H exhibits high absorption to short wavelengths (violet and blue light) and high transparency to the long wavelength (red light). In opposition, the back, thicker pin structure based on a-Si:H absorbs long wavelengths (red light), the green light is absorbed in both structures. The device selectivity is tuned externally using reverse bias (-8 V) and optical steady state illumination of short wavelength (400 nm). Exposed to light, the device offers high sensitivity and linear response, generating a proportional electrical current. Its quick response enables the possibility of high-speed communications. Since the photodetector response is insensitive to the frequency, phase, or polarization of the carriers, this kind of receiver is useful for intensity-modulated signals. The generated photocurrent is processed using a transimpedance circuit obtaining a proportional voltage. Since the photodetector response is insensitive to the frequency, phase, or polarization of the carriers, this kind of receiver is useful for intensity-modulated signals. After receiving the signal, it is in turn filtered, amplified, and converted back to digital format for demodulation. The system controller consists of a set of programmable modules.

In this system model, there are a few assumptions that should be noted: the channel state information is available both at the receiver and the transmitter; compared with the direct light, the reflected light is much weaker in the indoor VLC systems; only the Line OF Sight (LOS) path is considered and the multipath influence is not considered in the proposed indoor VLC system.

The received channel can be expressed as:

$$y = \mu h x + n \quad (1)$$

where y represents the received signal, x the transmitted signal, μ is the photoelectric conversion factor which can be normalized as $\mu = 1$, h is the channel gain and n is the additive white Gaussian noise of which the mean is 0.

The LEDs are modeled as Lambertian sources where the luminance is distributed uniformly in all directions, whereas the luminous intensity is different in all directions. The luminous intensity for a Lambertian source is given by Eq. (2) [15]:

$$I(\theta) = I_N \cos(\theta)^m \quad ; \quad m = \frac{\ln(2)}{\ln(\cos(\phi_{1/2}))} \quad (2)$$

I_N is the maximum luminous intensity in the axial direction, θ is the angle of irradiance and m is the order derived from a Lambertian pattern. For the proposed system, the commercial white LEDs were designed for illumination purposes, exhibiting a wide half intensity angle ($\phi_{1/2}$) of 60° . Thus, the Lambertian order m is 1. Friis' transmission equation is frequently used to calculate the maximum range by which a wireless link can operate. The coverage map is obtained by calculating the link budget from the Friis Transmission Equation [16]. The Friis transmission equation relates the received power (P_R) to the transmitted power (P_E), path loss distance (L_R), and gains from the emitter (G_E) and receiver (G_R) in a free-space communication link.

$$P_R [\text{dBm}] = P_E [\text{dBm}] + G_E [\text{dB}] + G_R [\text{dB}] - L_R [\text{dB}] \quad (3)$$

Taking into account Figure 2a, the path loss distance and the emitter gain will be given by:

$$L_R [\text{dB}] = 22 + 20 \ln \frac{d}{\lambda} \quad (4)$$

$$G_E [\text{dB}] = \frac{(m+1)A}{2\pi d_{E-R}^2} I(\theta) \cos(\theta) \quad (5)$$

With A de area of the photodetector and d_{E-R} the distance between each transmitter and every point on the receiver plane. Due to their filtering properties of the receptors the gains are strongly dependent on the wavelength of the pulsed LEDs. Gains (G_R) of 5, 4, 1.7 and 0.8 were used, respectively, for the R, G, B and V LEDs. I_N of 730 mcd, 650 mcd, 800 mcd and 900 mcd were considered.

Taking into account Equations (1)-(5), the coverage map for a square unit cell is displayed in Figure 3a. All the values were converted to decibel (dB).

On the receiving side, this is first done by a silicon carbide (SiC) pinpin MUX device that acts as an active filter for the visible region of the light spectrum. After receiving the signal, it is in turn filtered, amplified, and converted back to digital format for demodulation. The system controller consists of a set of programmable modules. To receive the I2V information from several transmitters, the receiver must be located at the overlap of the circles that set the transmission range (radial) of each transmitter. The coverage map for a square unit cell is displayed in Figure 3. The LEDs are modeled as Lambertian sources where the luminance is distributed uniformly in all directions, whereas the luminous intensity is different in all directions [15]. The nine possible overlaps (#1-#9), defined as fingerprint regions, as well as receiver orientations (2-9 steering angles; δ) are also pointed out for the unit square cell in Figure 3a.

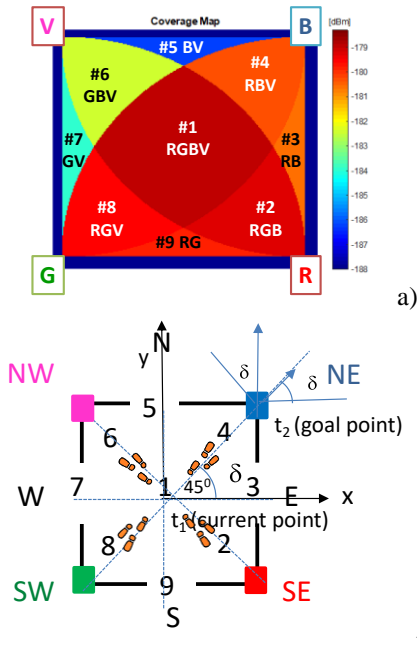


Figure 3. Illustration of: a) the coverage map in the unit cell. b) Footprint regions (#1-#9) and steering angle codes (2-9).

The input of the aided navigation system is the coded signal sent by the transmitters to an identify user, and includes its position in the network $P(x, y, z)$, inside the unit cell and the steering angle, δ , that guides the user across his path. The device receives multiple signals, finds the centroid of the received coordinates, and stores it as the reference point position. Nine reference points, for each unit cell, are identified giving a fine-grained resolution in the localization of the mobile device across each cell.

Along with the robustness of the electronic devices used, modulation is also paramount to ensure the VLC systems' performance and commercial viability. The core difference between VLC and regular RF (Radio-Frequency) communications is that VLC does not allow for amplitude and phase modulation techniques and must encode information by varying the intensity of emitted light.

An OOK modulation scheme was used to code the information. In OOK, the data bits are transmitted by having the LED illuminating at different intensity levels. For example, having the LED at its maximum brightness ("on") when transmitting the data bit '1' and dimmed ("off") when transmitting the data bit '0', this way digital data is represented by the presence or absence of a carrier wave. The main advantage of OOK is its simplicity and subsequent ease of implementation, whereas its main limiting factor are low data rates further exacerbated in systems using different dimming levels.

The obtained voltage is then processed, by using signal conditioning techniques (adaptive bandpass filtering and amplification, triggering and demultiplexing), until the data

signal is reconstructed at the data processing unit (digital conversion, decoding and decision) [14].

B. Architecture and Multi-person Cooperative Localization

Fog/Edge computing bridges the gap between the cloud and end devices by enabling computing, storage, networking, and data management on network nodes within the close vicinity of IoT devices. Fog computing has advantages since it provides moderate availability of computing resources at lower power consumption. Computing resources may be used for caching at the edge of the network, which enables faster retrieval of content and a lower burden on the front-haul. The edge is the immediate first hop from the IoT devices, such as the LiFi access points or gateways. In edge computing, the computation is done at the edge of the network through small data centers that are close to users. A mesh network is a good fit since it dynamically reconfigures itself and grows with the size of any installation. In Figure 4, the proposed architecture is illustrated.

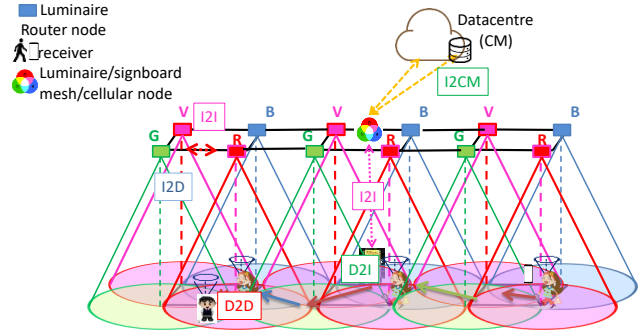


Figure 4. Mesh and cellular hybrid architecture.

The luminaires are equipped with one of two types of controllers: A "mesh" controller that connects with other nodes in its vicinity and can forward messages to other devices (I2D) in the mesh, effectively acting like routers nodes in the network. A "mesh/cellular" hybrid controller, that is also equipped with a modem providing IP base connectivity to the central manager services (I2CM). These nodes act as border-routers and can be used for edge computing. So, edge computing is located at the edge of the network close to end-user devices.

Under this architecture, the short-range mesh network purpose is twofold: enable edge computing and device-to-cloud communication, by ensuring a secure communication from a luminaire controller to the edge computer or datacenter (I2CM), through a neighbor luminaire/signboard controller with an active cellular connection; and enable peer-to-peer communication (I2I), to exchange information. It performs much of the processing on embedded computing platforms, directly interfacing to sensors and controllers. It

supports geo-distribution, local decision making, and real-time load-balancing. Moreover, it depends on the collaboration of near-located end-user devices, instead of relying on the remote servers, which reduces the deployment costs and delay.

C. Self-localization

Self-localization is a fundamental issue since the person must be able to estimate its position and orientation (pose) within a map of the environment it is navigating. We consider the path to be a geometric representation of a plan to move from a start pose to a goal pose (Figure 2). Let us consider a person navigating in a 2D environment. Its non-omnidirectional configuration is defined by position (x, y) and orientation angle δ , with respect to the coordinate axes. $q(t) = [x(t), y(t), \delta(t)]$ denote its pose at time t , in a global reference frame. In cooperative positioning systems, persons are divided into two groups, the stationary persons and the moving persons. Let us consider that $q_i(t, t')$ represents the pose of person i at time t' relative to the pose of the same person at time t and $q_{ij}(t)$ denotes the pose of person j relative to the pose of person i at time t . $q_i(t, t')$ is null for people standing still and non-zero if they move. These three types of information $q_i(t)$, $q_i(t, t')$ and $q_{ij}(t)$ compose the basic elements of a pose graph for multi-person cooperative localization.

We consider that the risk of virus transmission exists if $q_{ij}(t)$ is less than 2 m. The system will alert the users to stay away from those regions and to plan the better route to the desired wayfinding services. To estimate each person track the pure pursuit approach [17], [18] is used. The principle takes into account the curvature required for the mobile receiver to steer from its current position (t_1) to its intended position (t_2). By specifying a look-ahead distance, it defines the radius of an imaginary circle. Finally, a control algorithm chooses a steering angle in relation to this circle. This then allows to iteratively construct the intermediate arcs between itself and its goal position as it moved, thus, obtaining the required trajectory for it to reach its objective position. To avoid the risk of transmission, in the same frame of time and in known crowded regions, $q_{ij}(t)$ is estimated and the steering angle readjusted [19].

D. Scenario and building model

A navigation system refers to one that can identify the geographical coordinates of a user or device through a variety of data collecting mechanisms such as network routing addresses or geolocation devices. Once obtained, these coordinates determine the location of the user and allow them to “navigate” the map of an unfamiliar area by informing them of where they are, where their destination is, and step-by-step directions on what is the best route to get there. When it comes to outdoor positioning, the GPS (Global Positioning System) has been the most common means of identifying a user’s location, such as when driving

a vehicle. But when it comes to indoor navigation it is still far from maturity. The GPS cannot be relied on for this since satellite signals have trouble penetrating most buildings’ rooves, tunnels, or floors.

When utilizing a navigation system, users wish to be guided on a direct, shortest path, to their destination based on their current position (starting point) and where they wish to go (destination point). For this purpose, VLC utilizes cells for positioning along with a CM (Central Manager) to keep track of everything and generate the optimal path.

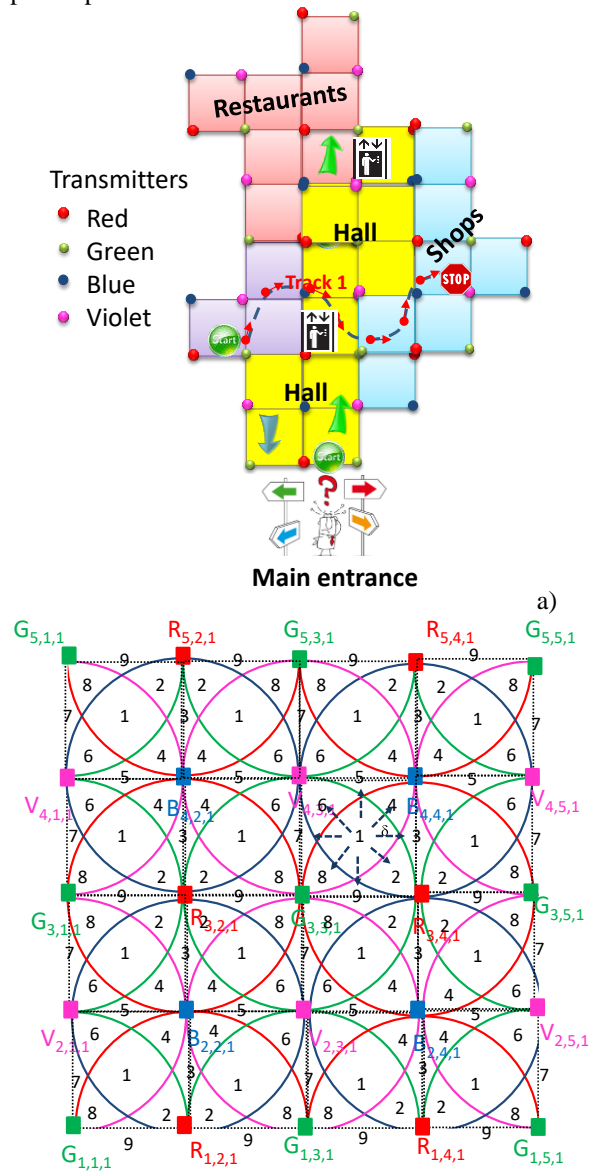


Figure 5. a) proposed scenario. b) Illustration of the 2D optical scenario (RGBV =modulated LEDs spots). Clusters of cells in square topology.

In VLC geotracking, geographic coordinates are generated, but the feature’s usefulness is enhanced by using them to determine a meaningful location, to guide the user through an unfamiliar building, or to lead him to his desired

meeting destination. It is believed this type of indoor location service would be most impactful in large-sized buildings with many points of interest and daily visitors, such as shopping malls and airports.

Building a geometry model of buildings' interiors is complex. Indoor VLC cell design is especially important since, being man-made, buildings such as these commonly follow basic shapes (squares, equilateral triangles/regular hexagons). In the proposed architecture each room/crossing/exit represents a node, and a path as the links between nodes. The proposed scenario is a multi-level building (Figure 5a). Lighting in large environments is designed to illuminate the entire space in a uniform way. Ceiling plans for the LED array layout, in floor level is shown in Figure 5b. A square lattice topology was considered for each level. A user navigates from outdoor to indoor. This topology is represented using x, y and z axes to simplify both the figure comprehension and the distance between any pair of nodes. In Figure 6 the 3D building model is depicted.

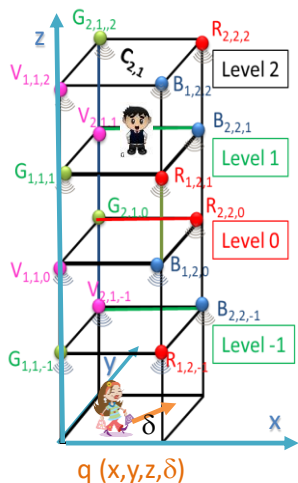


Figure 6. Illustration of the 3D optical scenario (RGBV=modulated LEDs spots). Row of cells in square topology.

Each node emits light all around it and up to a certain range, which allows each cell to be divided into footprints depending on which LEDs are covering any given space (Figure 3a), thus allowing the system to determine the position of a user or device in any given cell, $q(x,y,z,\delta)$.

A generated path to the end point can be viewed as a sequence of directions to nearby checkpoints that require the user to change their direction or steering angle (turning a corner, going around something, etc.). This means that a navigation system must also be able to identify the angle the user is moving in and the angle between the user and the next checkpoint (Figure 3b).

The user sends a request message to find the right track (D2I, in Figure 4) and, in the available time, he adds customized points of interest (wayfinding services). The requested information (I2D) is sent by the emitters at the

ceiling to its receiver. The indoor route throughout the building (track) is presented to the user by a responding message transmitted by the ceiling luminaires that work also either as router or mesh/cellular nodes. With this request/response concept, the generated landmark-based instructions help the user to unambiguously identify the correct decision point where a change of direction (pose) is needed, as well as offer information for the user to confirm that he/she is on the right way.

III. GEOTRACKING, NAVIGATION AND ROUTE CONTROL

Bi-directional communication between the infrastructure and the mobile receiver is analyzed.

A. Communication protocol and coding/decoding techniques

In order to ensure a synchronized and organized link between the user device and the various emitters, the use of a communication protocol for both encoding and decoding the shared data is important. To achieve this communication protocol, packets of bits are used, referred to as data frames, where its contents are formed from the required navigation data and arranged into several fields.

To code the information, an On-Off Keying (OOK) modulation scheme was used, and it was considered a synchronous transmission based on a 64- bits data frame.

Table 1. Frame structure

Header	Navigation Data					Payload		
	x	y	z	pin ₁	pin ₂	δ	Wayfinding data	Stop bit
5 bits (10101)	24 bits (4 bits per field)					34 bits (0 0)	1 bit (0)	
Frame length = 64 bits								

The frame is divided into three main blocks (Sync, Navigation data and Payload). The header block is the synchronization block [10101] This first block is named the header and refers to the starting bit sequence that is repeated in every data frame and allows the receiver to determine from an array of incoming bits where each frame begins. For this purpose, the same header bit sequence is imposed simultaneously to all emitters, in this case in an alternating “on”- “off” pattern [10101]. The second block contains the ID, 4+4+4 bits, gives the geolocation (x,y,z coordinates) of the emitters inside the array ($X_{i,j,k}$). These IDs were encoded using a 4-bit binary representation for the decimal number. The z coordinate refers to the floor number, which can be negative (ex: garages, machine rooms, warehouses, etc.) and is much less likely to reach double-digit values (skyscrapers being the most glaring exception); thus the first bit is used to represent the floor number's sign ('0' when a positive number, '1' when a negative number) and the remaining three bits indicating the coordinate's value.

When bidirectional communication is required, the user must register by choosing a username (pin_1) with 4 decimal numbers, each one associated to a RGBV channel. If buddy friend services are required a 4-binary code of the meeting (pin_2) must be inserted. The δ block (steering angle (δ)), a 4-bit sequence, completes the user's pose in a frame time $q(x, y, \delta, t)$. Eight steering angles along the cardinal points are possible from a start point to the next goal as pointed out as dotted arrows in Figure 5. The codes assigned to the pin_2 and to δ are the same in all the channels. If no wayfinding services are required these last three blocks are set at zero and the user only receives its own location.

The third and final block is named the payload and refers to sequence of bits that is not necessary for the navigation service. It is made up of miscellaneous data and followed by a stop bit. The frame payload starts with a sequence of bits that, while unnecessary for navigation, can be used to add more functionality to the indoor navigation service or even be used to improve the already existing one. The inclusion of a messaging service between users or a resending of one or more fields, are only two examples of how the payload can be used in a large-scale application.

Based on the measured photocurrent signal by the photodetector, it is necessary to decode the information received. A calibration curve is previously defined to establish this assignment. In Figure 7a, it is plotted the calibration curve that uses 16 distinct photocurrent thresholds resultant from the combination of the RGBV modulated signals from VLC emitter. The correspondence between each 4-binary code and the photocurrent level is highlighted on the right side. Here, the MUX signal obtained at the receiver as well as the coded transmitted optical signals is displayed. The message, in the frame, starts with the header labelled as Sync, a block of 5 bits. The same synchronization header [10101] is imposed simultaneously to all emitters. In the second block, labelled as calibration, the bit sequence was chosen to allow all the on/off sixteen possible combinations of the four RGBV input channels (2^4). Finally, a random message was transmitted [20]. Comparing the calibrated levels (d_0 - d_{15}) with the different assigned 4-digit binary [RGBV] codes, ascribed to each level, the decoding is straightforward, and the message decoded [21].

In Figure 7b, the MUX received signal and the decoding information that allows the VLC geotracking and guidance in successive instants (t_0 , t_1 , t_2) from user "7261" guiding him along his track is exemplified. The visualized cells, paths, and the reference points (footprints) are also shown as inserts. Data shows that at t_0 the network location of the received signals is $R_{3,2,1}$, $G_{3,1,1}$, $B_{4,2,1}$ and $V_{4,1,1}$, at t_1 the user receives the signal only from the $R_{3,2,1}$, $B_{4,2,1}$ nodes and at t_2 he was moved to the next cell since the node $G_{3,1,1}$ was added at the receiver. Hence, the mobile user "7261" begins his route into position #1 (t_0) and wants to be directed to his goal position, in the next cell (# 9). During the route the navigator is guided to E (code 3) and, at t_1 , steers to SE

(code 2), cross footprint #2 (t_3) and arrives to #9. The ceiling lamps (landmarks) spread over all the building and act as edge/fog nodes in the network, providing well-structured paths that maintain a navigator's orientation with respect to both the next landmark along the path and the distance to the eventual destination. Also, the VLC dynamic system enables cooperative and oppositional geolocation. In some cases, it is in the user's interest to be accurately located, so that they can be offered information relevant to their location and orientation (pin_1 , pin_2 and δ blocks). In other cases, users prefer not to disclose their location for privacy, in this case these last three blocks are set at zero and the user only receives its own location.

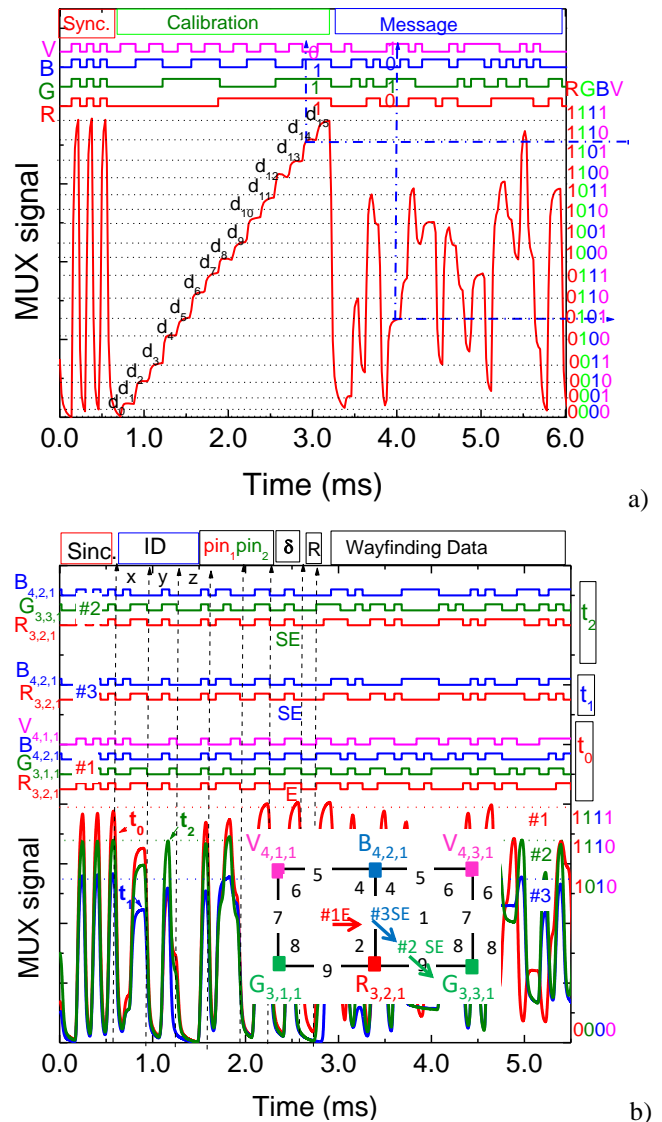


Figure 7. a) MUX/DEMUX signals of the calibrated cell. In the same frame of time a random signal (Message) is superimposed. b) Fine-grained indoor localization and navigation in successive instants. On the top the transmitted channels packets are decoded [R, G, B, V].

Due to the proximity of successive levels occasional errors occur in the decoded information. A parity check is performed after the word has been read [22]. The parity bits are the SUM bits of the three-bit additions of violet pulsed signal with two additional RGB bits and defined as:

$$P_R = V \oplus R \oplus B; P_G = V \oplus R \oplus G; P_B = V \oplus G \oplus B \quad (6)$$

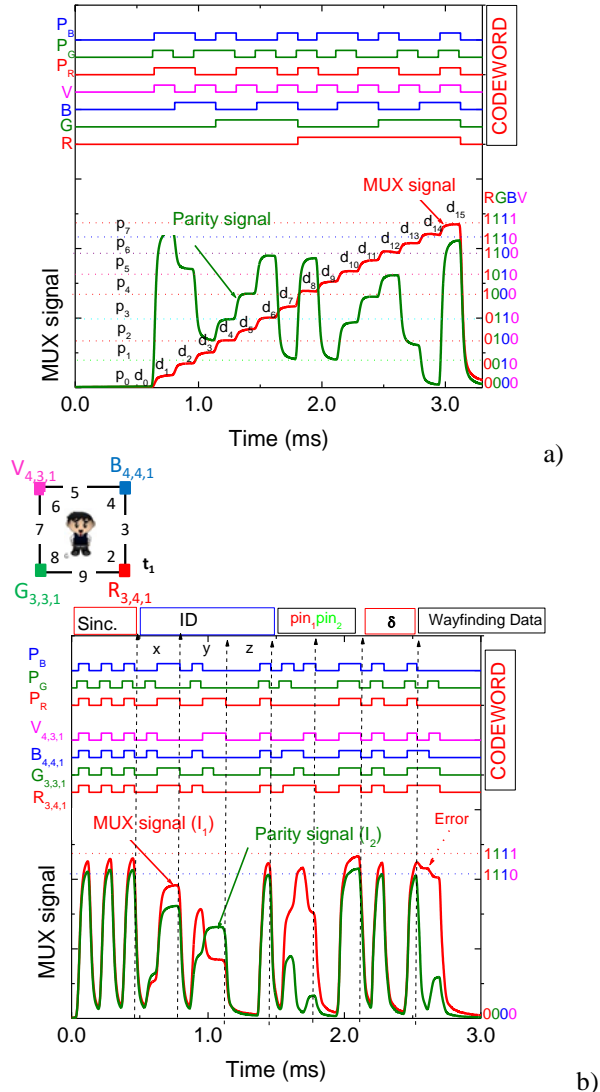


Figure 8. Code and parity MUX/DEMUX signals. On the top the transmitted channels [R G B V : P_R P_G P_B] are shown. a) Calibrated cell. b) Error control assigned to a request from user “7261” at C_{4,3,1}; #1 N.

In Figure 8a, the MUX signal that arises from the transmission of the four calibrated RGBV wavelength channels and the MUX signal that results from the generation of the synchronized parity MUX are displayed. On the top the seven bit word [R,G,B,V, P_R, P_G, P_B] of the transmitted inputs guides the eyes. The colors red, green, blue and violet were assigned respectively to P_R, P_G and P_B. For simplicity the received data (d₀₋₁₅ levels) is marked in

the correspondent MUX slots as well as the parity levels marked as horizontal lines. On the top the decoded 7-bit coded word is exhibited. In the right side 4-bit binary codes assigned to the eight parity sublevels are inserted.

The traffic message is revealed by decoding MUX signals and considering the framestructure, pose, and transmitter type [19]. In Figure 8b, we illustrate how error control is achieved using check parity bits. A request from user “7261” is shown at C_{4,3,1}; #1 N, along with the matching parity signal. Results show that without check parity bits, decoding was difficult primarily when levels were close together (dotted arrow).

The study of optical interference was also briefly attempted and how it can affect a VLC communication link. Three types of optical sources were chosen due to their availability and their likelihood of existing near a real-world indoor VLC system: halogen light, fluorescent light, and LED light. Measuring the intensity of each optical source at R (624 nm), G (540 nm), B (480 nm) and V (405 nm) wavelengths, without optical interference as a reference point, the RGBV (Red-Green-Blue-Violet) components of each optical source raises or lowers the light gain at those wavelengths. As the calibration curve is used to define the 16 possible levels (d₀-d₁₅, Figure 7), optical interferences are negligible. A wide range of factors influence optical interference (such as angle of incidence, optical aperture, luminous intensity, etc.) and, while some success has been observed in nullifying the disruptive effects of optical interference on decoding with the signal-to-bit algorithm, the results were based on specific optical sources measured under certain non-rigorous conditions. Before any concrete conclusions can be drawn about the full impact of optical interference on a VLC system and how it can be minimized or counteracted, further studies will be necessary to complement these results.

B. Multi-person cooperative localization and guidance services

Bi-directional communication between VLC emitters and receivers is available at a VLC ready handheld device, through the control manager interconnected with a signboard receiver located at each unit cells (#1). These communications channels constitute the uplink (D2I) and downlink channels (I2D). Each user (D2I) sends to the local controller a “request” message with the pose, $q_i(t)$, (x,y,z, δ), user code (pin₁) and also adds its needs (code meeting and wayfinding data). For route coordination the CM, using the information of the network’s VLC location capability, sends a personalized “response” message to each client at the requested pose with his wayfinding needs.

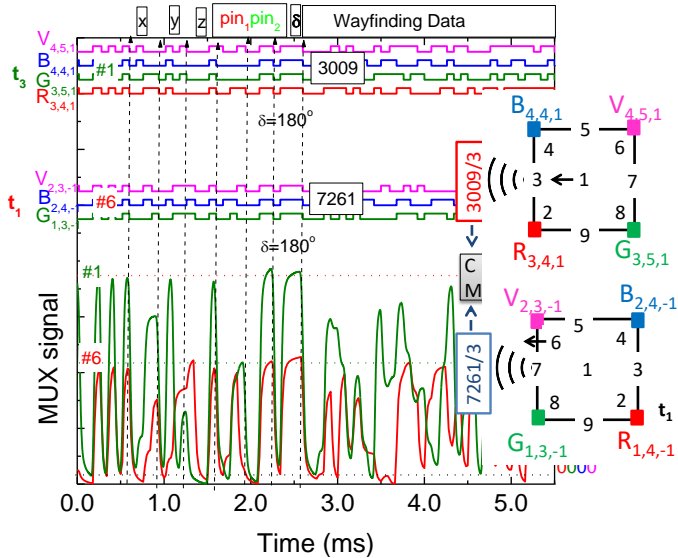


Figure 9. MUX/DEMUX signals assigned requests from two users (“3009” and “7261”) at different poses ($C_{4,4,1}$; #1W and $C_{2,3,-1}$; #6 W) and in successive instants (t_1 and t_3).

In Figure 9, the MUX synchronized signals received by two users that have requested wayfinding services, at different times, are displayed. We have assumed that a user located at $C_{2,3,-1}$, arrived first (t_1), auto-identified as (“7261”) and informed the controller of his intention to find a friend for a previously scheduled meeting (code 3). A buddy list is then generated and will include all the users who have the same meeting code. User “3009” arrives later (t_3), sends the alert notification ($C_{4,4,1}$; t_3) to be triggered when his friend is in his floor vicinity, level 1, identifies himself (“3009”) and uses the same code (code 3), to track the best way to his meeting.

After this request (t_3), the buddy finder service uses the location information from both user’ devices to determine the proximity of their owners ($q_{ij}(t)$) and sends a response message with the best route to the meeting.

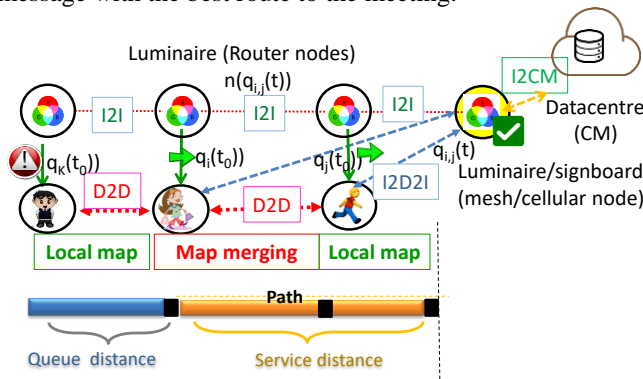


Figure 10. Graphical representation of the simultaneous localization and mapping problem using connectivity as a function of node density, mobility and transmission range.

The pedestrian movement along the path can be thought as a queue, where the pedestrians arrive at a path, wait if the

path is congested and then move once the congestion reduces.

In Figure 10, a graphical representation of the simultaneous localization and mapping problem using connectivity as a function of node density, mobility and transmission range is illustrated. The following parameters are therefore needed to model the queuing system: The initial arrival time (t_0) and the path, respectively, defined as the time when the pedestrian leaves the previous path and the actual movement along the path, $q_i(t, t')$. Here, the service time is calculated using walking speed and distance of the path.

The number of service units or resources is determined from the capacity of the path, $n(q_i(x,y,z, \delta, t))$ and walking speed that depends on the number of request services, and on the direction of movement along the path $q_i(x,y,z, \delta, t)$. Since the number of service units is same as the capacity of the path, the queue size is theoretically zero.

Once appended by the CM (request message), the pedestrians are served immediately (response message). If the number of pedestrians exceeds the path capacity, a backlog is automatically formed until the starting node. The hybrid controller integrates the number of requests and individual positions received during the same time interval. Once the individual positions are known, $q_i(t)$, the relative positions are calculated, $q_{ij}(t)$. If the relative position is less than a threshold distance, a crowded region locally exists, and an alert message is sent for the users. This alert allows the CM to recalculate, in real time, the best route for the users, $q_i(t, t')$, that request wayfinding services avoiding crowded regions.

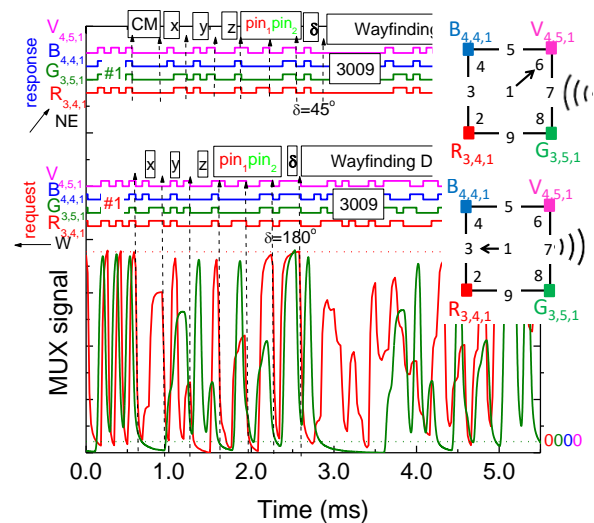


Figure 11. Request from user “3009” and response from the CM to him. On the top the transmitted channels packets are decoded $[X_{i,j,k}]$.

An example of the MUX signals assigned to a request/response received by user “3009” during his path to reach user “7261” is displayed in Figure 11. In the top of the

figure, the decoded information is shown and the simulated scenario is inserted to guide the eyes.

The “request” message includes, beyond synchronism, the identification of the user (“3009”), its address and orientation ($C_{4,4,1}$, #1W) and the help requested (Wayfinding Data). Since a meet-up between users is expected, its code was inserted before the right track request. In the “response”, the block CM identifies the sender [0000] and the next blocks the cell address ($C_{4,4,1}$), the user (3009) for which the message is intended and finally the requested information: meeting code 3, orientation NE (code 4) and wayfinding instructions. Every time a user switches floors he has to notify the CM and a new alert is received to optimize the way. In response to the estimated relative pose position, $q_{i,j}(t)$, between the users with the same meeting code, the CM sends a new alert that takes into account the occupancy of the service areas along the paths, $q_i(x,y,z, \delta, t)$, which optimizes the path without crowding the users.

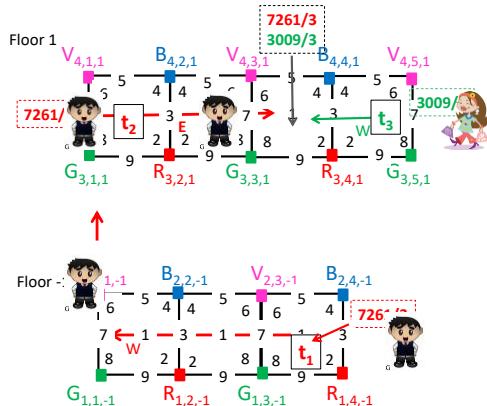
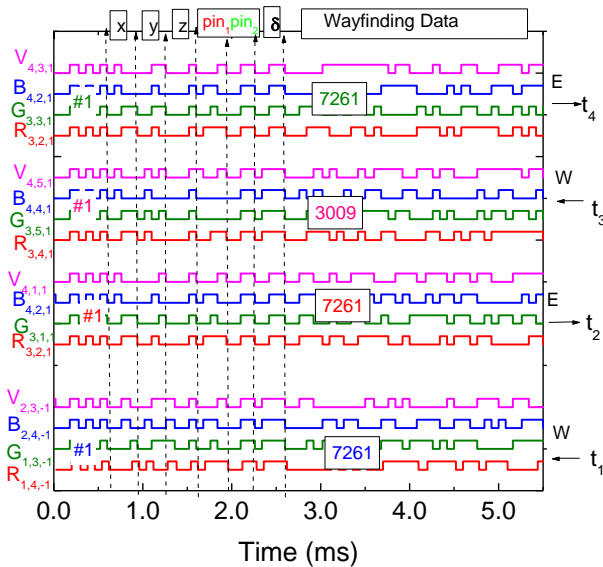


Figure 12. Decoded messages from the two users as they travel to a pre-scheduled meeting.

In Figure 12, the decoded messages from the two users as they travel to the pre-scheduled meeting is displayed. At the bottom the geolocation of both user is illustrated.

Decoded data shows that user “7621” starts (t_1) his journey on floor -1, $C_{2,3,-1}$; #1W, goes up to floor 1 in $C_{2,1,-1}$ and at t_2 he arrives at $C_{4,1,1}$ heading for E. During his journey, user “3009” from $C_{4,4,1}$ #1 asks the CM (t_3) to forward him to the scheduled meeting and follows course to W. At t_4 both friends join in $C_{4,3,1}$.

IV. CONCLUSIONS

A cooperative indoor VLC localization and navigation system is proposed. In a multi-level building scenario, the architecture of the system and the protocol of communication were defined. Bi-directional communication between the infrastructure and the mobile receiver was analyzed.

According to global results, the location of a mobile receiver is found in conjunction with data transmission. VLC's dynamic LED-aided navigation system is designed to give users accurate route guidance and enable navigation and geotracking. The multi-person cooperative localization system detects crowded regions and alerts the user to reschedule meetups, as well as provides guidance information. With those alerts, the CM can recalculate, in real time, the best route for users requesting wayfinding services, avoiding crowded areas.

ACKNOWLEDGEMENTS

This work was sponsored by FCT – Fundação para a Ciência e a Tecnologia, within the Research Unit CTS – Center of Technology and Systems, reference UIDB/00066/2020. The IPL/2022/POSEIDON_ISEL Project was also acknowledged.

REFERENCES

- [1] M. Vieira, M. A. Vieira, P. Louro, A. Fantoni, and P. Vieira, “Indoor Guidance Services through Visible Light Communication,” ALLSENSORS 2022: The Seventh International Conference on Advances in Sensors, Actuators, Metering and Sensing Copyright (c) IARIA, 2022. ISBN: 978-1-61208-987-4, pp. 8-12.
- [2] E. Ozgur E. Dinc, and O. B. Akan, “Communicate to illuminate: State-of-the-art and research challenges for visible light communications,” Physical Communication, vol. 17, pp. 72–85, 2015.
- [3] C. Yang and H. R. Shao, “WiFi-based indoor positioning,” IEEE Commun. Mag., vol. 53, no. 3, pp. 150–157, Mar. 2015.
- [4] D. Tsonev, et al. “A 3-Gb/s single-LED OFDM-based wireless VLC link using a Gallium Nitride μ LED,” IEEE Technol. Lett., vol. , no. 7, pp. 637–640, 2014.
- [5] D. O’Brien, et al., “Indoor visible light communications: challenges and prospects,” Proc. SPIE 7091, 709106, pp. 60–68, 2008.
- [6] H. -H. Liu and Y.-N Yang, ”WiFi-based indoor positioning for multi-floor environment,” Proceedings of the IEEE Region 10 Conference on Trends and Development in

- Converging Technology Towards (TENCON '11) November 2011 Bali, Indonesia 59760110.1109/TENCON.2011.61291752-s2.0-84863014825, pp.597-601, 2011.
- [7] Y. Wang, H. Li, X. Luo, Q. Sun, and J. Liu "A 3D Fingerprinting Positioning Method Based on Cellular Networks," *International Journal of Distributed Sensor Networks*, p. 248981, 2014.
- [8] M. Vieira, M. A. Vieira., P. Louro, P. Vieira, and A. Fantoni, "Fine-grained indoor localization: optical sensing and detection," *Proc. SPIE 10680, Optical Sensing and Detection V*, 106800H, 9 May 2018.
- [9] A. Jovicic, J. Li, and T. Richardson, "Visible light communication: opportunities, challenges and the path to market," *Communications Magazine, IEEE*, vol. 51, no. 12, pp. 26–32, 2013.
- [10] M. A. Vieira, M. Vieira, P. Louro, V. Silva, and P. Vieira, "Optical signal processing for indoor positioning using a-SiCH technology," *Opt. Eng.* Vol. 55, no. 10, 107105, 2016.
- [11] M. A. Vieira, P. Louro, M. Vieira, A. Fantoni, and A. Steiger-Garçon, "Light-activated amplification in Si-C tandem devices: A capacitive active filter model," *IEEE Sensor Journal*, 12, no. 6, pp. 1755-1762, 2012.
- [12] S. B. Park, et al., "Information broadcasting system based on visible light signboard," presented at *Wireless and Optical Communication 2007*, Montreal, Canada, 2007.
- [13] M. Vieira, M. A. Vieira, P. Louro, P. Vieira, and A. Fantoni, "Light-emitting diodes aided indoor localization using visible light communication technology," *Opt. Eng.*, vol. 57, no. 8, 087105, 2018.
- [14] M. A. Vieira, M. Vieira, P. Louro, and P. Vieira, "Bi-directional communication between infrastructures and vehicles through visible light," *Proc. SPIE 11207, Fourth International Conference on Applications of Optics and Photonics*, 112070C (3 October 2019); doi: 10.1117/12.2526500, 2019.
- [15] Y. Zhu, W. Liang, J. Zhang, and Y. Zhang, "Space-Collaborative Constellation Designs for MIMO Indoor Visible Light Communications," *IEEE Photonics Technology Letters*, vol. 27, no. 15, pp. 1667–1670, 2015.
- [16] H.T. Friis, "A note on a simple transmission formula" *Proc. IRE*34, pp. 254–256, 1946.
- [17] R. Rajesh, "Dynamic Vehicle and control" *Mechanical Engineering Series*, ISBN 978-1-4614-1433-9 . 2012.
- [18] J. Ackermann, J. Guldner, W. Sienel, R. Steinhauser, and V. Utkin, "Linear and Nonlinear Controller Design for Robust Automatic Steering," *IEEE Transactions on Control Systems Technology*, vol. 3, no. 1, pp. 132 – 143, Mar. 1995), DOI: 10.1109/87.370719, 1995.
- [19] M. Vieira, M. A. Vieira, P. Louro, A. Fantoni, and P. Vieira, "Geolocation and communication in unfamiliar indoor environments through visible light", *Proc. SPIE 11706, Light-Emitting Devices, Materials, and Applications XXV*, 117060P (March 2021); <https://doi.org/10.1117/12.2576904>.
- [20] M. Vieira, M. A. Vieira, P. Louro, A. Fantoni, P. Vieira, "Dynamic VLC navigation system in Crowded Buildings," *International Journal On Advances in Software*, vol. 14, no. 3&4, pp. 141-150, 2021.
- [21] M. Vieira, M.A. Vieira, P. Louro, P.Vieira, "A Visible Light Communication System to Support Indoor Guidance. In: Camarinha-Matos, L.M., Ribeiro, L., Strous, L. (eds) *Internet of Things. IoT through a Multi-disciplinary Perspective. IFIP IoT 2022. IFIP Advances in Information and Communication Technology*, vol 665, pp. 235-252. Springer, Cham. https://doi.org/10.1007/978-3-031-18872-5_14, 2022.
- [22] M. A. Vieira, M. Vieira, V. Silva, P. Louro, and J. Costa, "Optical signal processing for data error detection and correction using a-SiCH technology," *Phys. Status Solidi C*, vol. 12, no. 12, pp. 1393–1400, 2015.